$P2X_1$ ion channels promote neutrophil chemotaxis through Rho kinase activation[1]

Running title: $P2X_1$ ion channels contribute to neutrophil chemotaxis

Christelle Lecut,[2*] Kim Frederix,[2*] Daniel M. Johnson,[†] Christophe Deroanne,[‡] Marc Thiry,[§] Céline Faccinetto,[*] Raphaël Marée,[¶] Richard J. Evans,[‖] Paul G.A. Volders,[†] Vincent Bours,[*] Cécile Oury.[3*]

[*]GIGA-Research Human Genetics Unit, [‡]GIGA-Research Laboratory of connective tissue biology, [§]Cellular Biology Unit, [¶]GIGA Bioinformatics Platform, University of Liège, Belgium.

[†]Department of Cardiology, Cardiovascular Research Institute Maastricht, The Netherlands.

[‖]Department of Cell Physiology and Pharmacology, University of Leicester, United Kingdom.

Keywords: Neutrophils, chemotaxis, human, transgenic/knock-out mice, signal transduction

Abstract (228)

Adenosine 5'-triphosphate (ATP), released at the leading edge of migrating neutrophils, amplifies chemotactic signals. The aim of our study was to investigate whether neutrophils express ATP-gated $P2X_1$ ion channels and whether these channels could play a role in chemotaxis. Whole-cell patch clamp experiments showed rapidly desensitizing currents in both human and mouse neutrophils stimulated with $P2X_1$ agonists, alpha,beta-methylene ATP (αβMeATP) and beta,gamma-methylene ATP (βγMeATP). These currents were strongly impaired or absent in neutrophils from $P2X_1^{-/-}$ mice. In Boyden chamber assays, αβMeATP provoked chemokinesis and enhanced formylated peptide- and interleukin-8-induced chemotaxis of human neutrophils. This agonist similarly increased W-peptide-induced chemotaxis of wild-type mouse neutrophils while it had no effect on $P2X_1^{-/-}$ neutrophils. In human as in mouse neutrophils, αβMeATP selectively activated the small RhoGTPase RhoA that caused reversible myosin light chain phosphorylation. Moreover, the αβMeATP-elicited neutrophil movements were prevented by the two Rho kinase inhibitors, Y27632 and H1152. In a gradient of W-peptide, $P2X_1^{-/-}$ neutrophils migrated with reduced speed and displayed impaired trailing edge retraction. Finally, neutrophil recruitment in mouse peritoneum upon *E. coli* injection was enhanced in wild type mice treated with αβMeATP while it was significantly impaired in the $P2X_1^{-/-}$ mice. Thus, activation of $P2X_1$ ion channels by ATP promotes neutrophil chemotaxis, a process involving Rho kinase-dependent actomyosin-mediated contraction at the cell rear. These ion channels may therefore play a significant role in host defense and inflammation.

Introduction

Neutrophils are key cells of the innate immune system that participate in a vast majority of inflammation-related diseases, such as coronary artery diseases, rheumatoid arthritis, and sepsis (1-3). They are programmed to exit the circulation and chemotax toward epicentres of inflammation, guided by gradients of a variety of inflammatory mediators (4). Neutrophils become polarized morphologically in response to chemotactic stimuli. These morphological changes are accompanied by a strongly polarized distribution of intracellular signal transduction components. 3'-phosphoinositol lipids (PI3Ps) and phosphoinositide-3'-kinases (PI3Ks), Rho GTPases, such as RhoA, Rac, and Cdc42, and the actin and microtubule cytoskeletons play key roles in signaling polarity. Attractant receptors, acting on different G proteins, trigger two divergent pathways that contribute to polarity (5). Frontness depends upon Gi-mediated production of PI3Ps, the activated form of Rac, and F-actin. G12 and G13 trigger backness signals, including activation of Rho, a Rho-dependent kinase, and myosin II. Functional incompatibility causes the two resulting actin assemblies to aggregate into separate domains, making the leading edge more sensitive to attractant than the back (5).

In addition, mechanisms of signal amplification have been proposed that contribute to maintain signaling polarity even in a shallow gradient. These mechanisms involve the release of ATP from neutrophil leading edge and its rapid metabolism to ADP, AMP and adenosine (6). As a neutrophil moves toward an attracting stimulus, a rapid and transient release of ATP further enforces its directional movement by autocrine signaling via $P2Y_2$ and A3 receptors. In support of this, neutrophils lacking $P2Y_2$ receptors showed a loss in gradient sensing, whereas cells without A3 receptors showed correct directionality but diminished speed (6). Although the intracellular mechanisms remain undefined, these findings demonstrate the importance of extracellular ATP in the control of neutrophil chemotaxis.

Because ATP is released by activated platelets and leukocytes, as a result of multiple stress stimuli, and upon cell lysis, its concentration can become elevated at sites of inflammation (7). By acting on neutrophils in a paracrine manner, ATP could thus help these cells to locate bacteria and tissue damage. We therefore wondered whether neutrophils expressed other ATP receptors that could contribute to chemotaxis. ATP acts on specific cell surface P2 receptors belonging to two subclasses, the G protein-coupled P2Y receptors and the ATP-gated P2X non-selective cation channels (8, 9). Eight human P2Y receptors, $P2Y_1$, $P2Y_2$, $P2Y_4$, $P2Y_6$, $P2Y_{11-14}$, and seven P2X subtypes, $P2X_{1-7}$, have been identified (9-11). Neutrophils express multiple P2X subtype mRNAs: $P2X_{1,4,5,7}$ (6, 12-14). However, the presence of functional P2X ion channels in neutrophils has never been shown and their contribution to neutrophil migration has never been investigated. P2X ion channels are widely distributed in various cell types and tissues (15). Only $P2X_7$ receptors are thus far established as having physiological roles in inflammation, mostly via a rapid activation of caspase-1 with subsequent release of the proinflammatory cytokine IL-1β from activated macrophages and microglia (15, 16). $P2X_7$ is also an important modulator of T cell functions (17-20).

In this study, we demonstrate that both human and mouse neutrophils express $P2X_1$ ion channels that play a significant role in the neutrophil response to chemotactic stimuli.

Materials and Methods

Reagents

α,β-methylene ATP (αβMeATP), β,γ-Methylene ATP (βγMeATP), fMLP, BSA were from Sigma-Aldrich (Bornem, Belgium). W-peptide was from Innovagen (Lund, Sweden). Mouse type IV collagen was from BD Biosciences (Erembodegem, Belgium). Home-made polyclonal rabbit anti-$P2X_1$ antibody was described previously.(21) Polyclonal goat anti-myosin light chain (MLC)2 and anti-phospho MLC (Thr18/Ser19), mouse anti-RhoA, and mouse anti-Rac2 antibodies were from Santa-Cruz (Santa Cruz, CA). Mouse anti-Rac1 (23A8) was from Upstate Biotechnology (Heule, Belgium). Mouse anti-Cdc42 was from BD Biosciences (Erembodegem, Belgium). AlexaFluor488-coupled phalloidin was from Invitrogen (Merelbeke, Belgium).

Mice

Animals used in this study were 8-12 week-old C57BL/6 mice (wild-type and $P2X_1^{-/-}$ described previously (22)) that were housed in specific pathogen-free animal facilities. All experiments were carried out following the guidelines of and in agreement with the local ethic committee.

Human neutrophil isolation

Fresh acid-citrate-dextrose (ACD; 93 mM sodium citrate, 7 mM citric acid, 0.14 mM dextrose, pH 6.5)-anticoagulated peripheral blood was drawn by venipuncture from healthy volunteers. Institutional Review Board approval was obtained from the Centre Hospitalier Universitaire de Liège, and informed consent from volunteers was obtained in accordance

with the Declaration of Helsinki. Neutrophils were isolated by plasma/percoll gradient centrifugation mainly as previously described (23).

Mouse peritoneal neutrophil isolation

Mice were injected intraperitoneally with 500µl 4% thioglycollate in PBS. Three hours after injection, peritoneal lavage was performed with 5 ml ice-cold PBS. Neutrophils were isolated by positive magnetic selection using an anti-Gr1 antibody (Miltenyi Biotec, Utrecht, The Netherlands). Cells were counted and resuspended at a density of 1 X 10^6 cells/ml in HBSS containing 1 mM $CaCl_2$, 2 mM $MgCl_2$ and 0.2% BSA (referred as to HBSS buffer).

Western blotting

Western blotting detection of $P2X_1$, phospho-MLC, and MLC proteins in neutrophil extracts was performed as previously described (24-26). For phospho-MLC, and MLC detection, neutrophils were treated with 2.7 mM diisopropyl fluorophosphate for 15 min prior to stimulation with agonist for indicated times.

Rho GTPases pull-down assays

After pretreatment with 2.7 mM diisopropyl fluorophosphate for 15 min, neutrophils were stimulated with αβMeATP for the indicated times. Reaction was stopped by lysing the cells in the following ice-cold buffer: 0.5% Triton X-100, 25 mM HEPES, pH 7.3, 150 mM NaCl, 5mM $MgCl_2$, 0.5mM EGTA, 5 mM DTT, 4% glycerol, containing Complete protease inhibitors, 10 mM sodium fluoride, 2 mM β-glycerophosphate, 2 mM sodium orthovanadate and 1 mM phenylmethylsulphonyl fluoride. Lysates were centrifuged for 8 min at 13,000*g*. An aliquot of each supernatant was denatured in Laemmli buffer to measure the total RhoGTPase content by Western blotting. For pull-down assays, supernatants were incubated

for 30 min with 30 µg of GST-PBD protein containing the Cdc42 and Rac binding region of PAK-1B, or GST-RBD protein containing the Rho binding region of rhotekin affinity linked to glutathione-Sepharose beads. The beads were washed four times in lysis buffer and boiled in Laemmli buffer. Lysates were loaded on SDS-PAGE and Western blotting was performed (25).

Electrophysiology

During isolation, both murine and human neutrophils were treated with 15U/ml apyrase (Grade I, Sigma-Aldrich) to remove extracellular ATP and prevent $P2X_1$ desensitization. Isolated neutrophils were adhered on a tissue culture dish and placed in a perfusion chamber on an inverted microscope that was continuously perfused with external solution containing 147 mM NaCl, 3 mM KCl, 2 mM $CaCl_2$, 10 mM HEPES, and 13 mM glucose (pH = 7.4 with NaOH). Whole cell patch clamp recordings were made at room temperature (23 ± 1°C) using an Axopatch-1D amplifier and pCLAMP8 software (Axon Instruments, Union City, CA). Pipette resistances ranged from 5 to 12 MΩ when filled with internal solution containing 147 mM NaCl, 10 mM EGTA, and 10 mM HEPES (pH 7.3 with NaOH). Gigaseals were obtained and currents were sampled at 10KHz after low-pass filtering at 1KHz. Series resistance was not routinely compensated. The membrane potential was clamped at –70 mV throughout the experiments. Fast solution changes were achieved with the complete VC-6 fast-step perfusion system (Harvard apparatus) together with a multi-barrel glass pipette that was positioned about 50 µm from the cell during drug application. Analysis of data was achieved with Clampfit 8.0 (Axon Instruments, Union City, CA) and Prism 4.0 (Graphpad, Software Inc., San Diego, CA).

Boyden Chamber assays

48-well microchemotaxis plates (Neuro Probe Inc., Gaithersburg, MD) and 8 µm (human neutrophils) or 5 µm (mouse neutrophils) pore-size polyvinylpyrrolidone-free polycarbonate membranes (VWR, Leuven, Belgium) were used. Chemoattractant diluted in HBSS buffer was placed in the chamber bottom wells, and neutrophil suspension (1 X 10^6 cells/ml) was added to the top wells. HBSS buffer was used as a negative control. The plate was incubated for 1 hour at 37°C. Membrane was removed, fixed and stained using a Diff-Quick stain set (Medion diagnostics, Düdingen, Switzerland). The number of neutrophils that migrated to the lower side of the membrane was counted in ten random microscope fields using the 40X objective (Olympus BHB, Aartselaar, Belgium). The chemotactic index is defined as follows: (mean neutrophils per field in chemoattractant – mean neutrophils per field in HBSS) / mean neutrophil per field in HBSS).

F-actin staining and confocal microscopy

Murine peritoneal neutrophils (1.10^6/ml in HBSS buffer) were let to adhere on collagen type IV-coated microslides (Ibidi, Integrated BioDiagnostics, Martiensried, Germany) for 15 minutes at room temperature. Neutrophils were incubated with 100nM W-peptide for the indicated times, before fixation in 4% paraformaldehyde. Cells were incubated in HBSS containing 0.25% triton-X100, 2% BSA and AlexaFluor488-coupled phalloidin. Microslides were analyzed with a Leica TCS SP2 confocal microscope equipped with a 63x objective (Leica Microsystems Heidelberg GmbH).

Time-lapse video microscopy: chemotaxis microslides

Chemotaxis microslides coated with type IV collagen or fibronectin (Ibidi, Martiensried, Germany) were used to study two-dimensional neutrophil migration. Murine neutrophils (3 X 10^6 cells/ml in HBSS buffer) were adhered to coated-microslides for 15 min at RT. Microslide

reservoirs were then filled with buffer, and chemoattractant was added. After 15 min, to allow diffusion of the chemoattractant and establishment of a linear gradient, neutrophil migration was observed using a Nikon Eclipse TS100 inverted microscope, equipped with a Nikon digital sight DS-2Mv camera. The Basic Research NIS-Elements Imaging software (Nikon) was used for time-lapse imaging. Phase contrast images were captured every minute. Cell-tracking software (Chemotaxis and Migration Software tool based on ImageJ, Ibidi) was used to characterize chemotaxis from the captured images. The average circularity ratio of cells is a well-known compactness measure of a shape computed by ImageJ and defined as $C = 4\pi$ (area) / (perimeter)^2. For a perfect circle C equals 1 whereas for a long, thin shape, C tends to 0. This ratio was computed for each cell at each capture by successively applying the Canny edge detector using FeatureJ plugin, thresholding using the Isodata algorithm, and morphological operations (fill holes, erosion, and dilation). Parameter default values were used for all experiments.

Static adhesion assay

96-well culture plates were coated with mouse type IV collagen (40µg/ml). Neutrophils from wild-type or $P2X_1^{-/-}$ mice were allowed to adhere to collagen for 15 min at 37°C. Unattached cells were gently removed and wells were rinsed once with HBSS buffer. Neutrophil adhesion was determined using the CellTiter-Glo luminescent cell viability assay (Promega, Leiden, The Netherlands). Luminescence was measured in a Victor2 multilabel microplate reader (Perkin Elmer).

Mouse peritonitis model

Wild-type mice (n=4-6 mice per group, 3 independent experiments) were intraperitoneally injected with 100 µl αβMeATP (0.16µmol/kg) or vehicle 15 min before intraperitoneal

injection of 150 µl of *E. coli* (ATCC 25922) (50 X 10^6 colony forming units/ml) or PBS. Mice were then injected with 100 µl αβMeATP after 1 and 2 hours. For experiments with $P2X_1^{-/-}$ mice, animals were injected once with 150 µl of *E. coli* or PBS. After 3 hours, the mice were killed, and peritoneal exudate cells were harvested by 5 successive washes with 1 ml PBS containing 0.5% BSA and 2 mM EDTA. Total amounts of peritoneal cells were counted and differential cell counts were determined by microscopic analysis of Giemsa-Wright–stained cytospins.

Statistics

Data are represented as mean ± SD of at least 3 independent experiments. Statistical analyses were performed using either Student's t-test or, for multiple comparisons, one-way ANOVA followed by the Bonferroni's test.

Results

Human neutrophils express functional $P2X_1$ channels.

In agreement with previous studies (6, 13), real time RT-PCR analyses indicated that human peripheral neutrophils mainly expressed $P2X_1$ subtype mRNAs (data not shown). Lower levels of $P2X_4$, $P2X_5$ and $P2X_6$ mRNA subtypes were also detected. We assessed whether $P2X_1$ proteins were expressed in neutrophil membranes and formed functional ion channels. Expression of $P2X_1$ proteins was analyzed by Western blotting (Fig. 1A). The apparent molecular weight of neutrophil $P2X_1$ proteins was about 60 kD, similar to that of the glycosylated form of platelet $P2X_1$ (27). Functionality of the $P2X_1$ ion channels was studied by whole-cell patch clamp analyses. Application of the $P2X_1$ selective agonist αβMeATP (10 μM) induced rapidly desensitizing inward currents of about 40 pA/pF (Fig. 1B). Currents of lower density (20 pA/pF) were observed upon application of the same concentration of the other $P2X_1$ agonist, βγMeATP, which is consistent with $P2X_1$ pharmacological properties described in other cell types (28, 29). Moreover, applying ATP (100 μM) gave rise to similar rapidly desensitizing currents (data not shown), suggesting that human neutrophils do not express functional P2X ion channels characterized by slow desensitization kinetics (composed of $P2X_4$, $P2X_5$ and/or $P2X_6$ subunits).

αβMeATP induces random migration and enhances chemotaxis of human peripheral neutrophils.

The effect of αβMeATP on neutrophil chemotaxis was investigated using Boyden chamber assays (30) (Fig. 2A). We placed neutrophils into the chamber top wells and allowed them to migrate in the bottom wells. αβMeATP (10 μM), placed in the bottom wells, did not induce significant neutrophil chemotaxis. However, pretreating neutrophils with αβMeATP

significantly increased chemotactic index (CI). In the absence of αβMeATP in the bottom wells, the migratory activity of αβMeATP-treated neutrophils also tended to be augmented. Similar results were obtained when βγMeATP was used as $P2X_1$ agonist (data not shown). Neutrophils chemotaxed efficiently in response to interleukin-8 (CI=10.5) (Fig. 2B). We found that pretreating the cells with αβMeATP markedly enhanced chemotaxis induced by IL-8 (CI=32.6) (Fig. 2B), at any tested IL-8 concentration (from 10 to 500 ng/ml) (data not shown). A similar phenomenon was observed when formylated peptide (fMLP, 100 nM) was used as chemoattractant (Fig. 2C). Only short treatment with the agonist (around 1 min) led to the increased chemotaxis (supplemental Fig. S1C).[5] When longer pre-incubation periods were used (from 5 min), αβMeATP failed to enhance neutrophil migration, pointing to the importance of the kinetics of $P2X_1$-mediated signaling. Thus, stimulation of neutrophils with $P2X_1$ agonists promoted neutrophil chemotaxis in response to both endogenous (IL-8) and exogenous bacterial (fMLP) chemoattractant. The αβMeATP-induced increase of chemotaxis toward fMLP was fully inhibited by the selective $P2X_1$ antagonist, NF449, and was similar to the effect of the nonhydrolyzable ATP analog adenosine 5'-O-(3-thiotriphosphate) (ATP-γ-S) (supplemental Fig. S1A,B).[5] ATP was more potent to enhance migration than the two analogs, possibly because of ATP conversion to adenosine during cell migration (supplemental Fig. S1B).[5] Strikingly, the addition of αβMeATP in the chemoattractant medium failed to increase chemotaxis (Fig. 2D). Taken together, these results indicated that αβMeATP was not chemotactic by itself but could induce random neutrophil migration (chemokinesis). This is in sharp contrast with the effect of the $P2Y_2$ receptor agonist, UTP, that was able to increase fMLP-induced chemotaxis when added together with fMLP in the bottom wells of the Boyden chamber, as well as when it was placed in direct contact with the cells (Fig. 2E).

αβMeATP-induced migration involves the Rho pathway

We then investigated the molecular mechanisms underlying the αβMeATP-induced migration**.** In order to analyze the activity of Rho GTPases, central players in signaling polarity during cell migration (4), we performed GST-pull down assays using lysates of αβMeATP-stimulated human neutrophils.

We found that αβMeATP (10 μM) rapidly and selectively activated RhoA (Fig. 3). The amount of GTP-bound RhoA increased by 4.2 ± 0.4, 4.1 ± 1.4 and 3.7 ± 1.7 fold after 10 s, 30 s, and 1 min of stimulation, respectively. In contrast, αβMeATP failed to activate Rac1, Rac2 or Cdc42 (Fig. 3B). Consistently with the activation of the Rho pathway, we also found that αβMeATP increased myosin light chain (MLC) phosphorylation, being maximal after 1 min and disappearing after 5 min (Fig. 3C).

To determine whether the Rho pathway was involved in αβMeATP-induced chemokinesis, neutrophils were incubated with two different inhibitors of the Rho kinase, Y27632 and H1152, and Boyden Chamber assays were performed. Both inhibitors fully blocked neutrophil migration induced by αβMeATP (Fig. 3D). Under our experimental conditions, Y27632 (5 μM) alone failed to inhibit chemotaxis toward fMLP whereas it abolished the effect of αβMeATP (Fig. 3E). On the contrary, inhibiting PI3Kγ with AS252424 (31, 32) failed to modify αβMeATP-triggered chemokinesis (data not shown) whereas it totally blocked the fMLP-induced chemotaxis (data not shown). Taken together, these results indicate the involvement of the RhoA/Rho Kinase pathway in $P2X_1$-mediated neutrophil chemokinesis.

Characterization of $P2X_1^{-/-}$ neutrophils

To further characterize $P2X_1$ function in neutrophil chemotaxis and to assess agonist specificity, we used cells isolated from $P2X_1^{-/-}$ mice.(22) The hematological profile of these mice has been analyzed in a previous study, revealing normal erythrocyte and leukocyte counts, hemoglobin and hematocrit (33). The distribution of leukocyte cell types was also

similar between wild-type and knock-out mice. In transmission electron microscopy, we showed that $P2X_1^{-/-}$ peripheral neutrophils had no apparent ultrastructural abnormalities (data not shown). We then performed whole-cell patch clamp experiments on mouse peritoneal neutrophils. As observed in human cells, neutrophils from wild-type mice displayed rapidly desensitizing inward currents upon stimulation with the two $P2X_1$ agonists, αβMeATP (10 μM) and βγMeATP (10 μM). Current density was 136.9 ± 44.9 pA/pF and 51.6 ± 22.1 pA/pF (means ± SEM), respectively (Fig. 4). βγMeATP-induced currents were absent in $P2X_1^{-/-}$ neutrophils. A remaining rapidly desensitizing current could still be induced by αβMeATP in cells lacking $P2X_1$ (mean current density = 70.7 ± 20.2 pA/pF). $P2X_1$ characteristics (sensitivity to activation by αβMeATP and rapid desensitization kinetics) are shared by $P2X_3$ homomeric channels (28). While βγMeATP is reported to be equipotent to αβMeATP at $P2X_1$, it is approximately 30-to 50-fold less potent at $P2X_3$. Real time RT-PCR analyses indicated that, in contrast to human neutrophils, mouse neutrophils expressed $P2X_3$ subtype mRNAs (data not shown). $P2X_3$ channels might thus mediate the residual αβMeATP-induced current in $P2X_1^{-/-}$ neutrophils.

We then investigated the chemotactic properties of $P2X_1^{-/-}$ neutrophils *in vitro*. We first used Boyden chamber assays to assess direction sensing (30). Migration toward the chemotactic peptide W-peptide was similar for both $P2X_1^{-/-}$ and wild-type neutrophils (Fig. 5A), and about 10 fold higher than toward the HBSS buffer control (data not shown). This indicated that $P2X_1$ was not required for direction sensing. Nevertheless, pretreating wild-type neutrophils with αβMeATP (10 μM) significantly enhanced W-peptide-induced chemotaxis (Fig. 5A), as observed for human neutrophils. The migratory activity of $P2X_1^{-/-}$ cells was not affected by αβMeATP (Fig. 5A), demonstrating that the αβMeATP effects on migration require $P2X_1$ ion channels.

As observed for human cells, $P2X_1$-mediated neutrophil migration also involved the Rho pathway in murine neutrophils. In Boyden chamber assays, the enhancing effect of αβMeATP on W-peptide-induced migration of wild-type neutrophils was fully blocked when cells were pre-treated with inhibitors of the Rho Kinase (Figure 5B). Using GST-pull down assays, we found that $P2X_1$ activation with αβMeATP was able to rapidly increase RhoA activity in wild-type neutrophils whereas RhoA activity in $P2X_1^{-/-}$ neutrophils was not affected by this agonist (Figure 5C).

Reduced speed and static adhesion for $P2X_1^{-/-}$ neutrophils

We next investigated two-dimensional chemotaxis of $P2X_1^{-/-}$ neutrophils using Ibidi chemotaxis microslides and time-lapse video microscropy. Mouse peritoneal neutrophils were adhered on collagen type IV and placed in a gradient of W-peptide. Both wild-type and $P2X_1^{-/-}$ neutrophils migrated toward the W-peptide gradient (supplemental videos 1 and 2)[5]. Cell tracking showed that the forward migration index determined for $P2X_1^{-/-}$ neutrophils was comparable to the one of wild-type cells, indicating that neutrophils can orient normally in the absence of $P2X_1$. Nevertheless, further analyses revealed diminished migration speed for $P2X_1^{-/-}$ neutrophils (Fig. 6A). The addition of the ATP/ADP scavenger, apyrase, reduced the migration speed of wild-type neutrophils to a similar extent as for $P2X_1^{-/-}$ cells, pointing to a contribution for ATP released by migrating cells during the assays (supplemental Fig. S2B).[5] A reduced migration speed was also observed when $P2X_1^{-/-}$ neutrophils were adhered to fibronectin (supplemental Fig. S2A),[5] indicating that this defect was not substrate-specific. Moreover, the detachment of fine trailing appendages at the rear of $P2X_1^{-/-}$ neutrophils appeared to be delayed as compared to wild-type cells (Fig. 6B). Among 80 cells analyzed, 75% of $P2X_1^{-/-}$ neutrophils showed a tail persisting for 45 min whereas this percentage was 16.7% for wild-type cells (46.7% of the wild-type cells displayed a tail persisting for 31 to 45

min, and 23.3% for 16 to 30 min). To support these observations, we quantified cell deformation during the time course of the experiments. For this purpose, we calculated circularity ratios for all cells (see Material and Methods). During migration of wild-type neutrophils, quite constant and repetitive oscillations of the averaged ratios occurred (representing cell deformation) but the cells always recovered their original shape (Fig. 6C). Notably, although such oscillations were also observed for $P2X_1^{-/-}$ neutrophils, from about 35 min of migration up to 60 min, the shape of these cells remained thinner and longer than at earlier time steps, possibly reflecting an impaired trailing edge retraction. Furthermore, static adhesion of $P2X_1^{-/-}$ neutrophils to collagen IV was found to be reduced by about 30% (Fig. 6D). Thus, activation of $P2X_1$ by released ATP could promote cell movement during chemotaxis, facilitating cell deformation and adhesion dynamics. In agreement with the Boyden chamber assays, $P2X_1$ would not contribute to cell orientation (gradient sensing). In order to determine whether $P2X_1$ would be involved in actin cytoskeleton reorganization in migrating neutrophils, we performed F-actin staining in WT and $P2X_1^{-/-}$ neutrophils uniformly stimulated with W-peptide. Polarized actin polymerization appeared to occur normally in cells lacking $P2X_1$ (Fig. 7).

$P2X_1$ activation promotes neutrophil recruitment in vivo in a peritonitis model

The role of $P2X_1$ in neutrophil chemotaxis was further investigated *in vivo* by assessing cell recruitment in the peritoneal cavity of mice intraperitoneally injected with living *E. coli* bacteria. αβMeATP-treated mice showed significantly increased numbers of neutrophils in the peritoneum as compared to untreated animals (Fig. 8A), indicating that $P2X_1$ activation promotes bacteria-induced neutrophil recruitment *in vivo*. Accordingly, we found that *E.coli*-induced neutrophil recruitment was impaired in the $P2X_1^{-/-}$ mice as compared to wild-type animals (Fig 8B).

Discussion

Our data demonstrate for the first time that human and mouse neutrophils express functional $P2X_1$ ion channels. Whole-cell patch clamp revealed that two $P2X_1$ agonists evoked rapidly desensitizing inward currents that were absent (βγMeATP) or impaired (αβMeATP) in neutrophils isolated from $P2X_1^{-/-}$ mouse peritoneum.

Our work significantly extends the knowledge on $P2X_1$ expression in various blood cell types. In platelets, $P2X_1$, strongly expressed as a heavily glycosylated protein (27), contributes to thrombus formation under high shear stress conditions and has been proposed to be an interesting new target for antithrombotic drugs (24, 33, 34). Previous studies of $P2X_1$ receptor expression in other human hematopoietic cell types have reported $P2X_1$ receptor mRNA in total human blood leukocytes (35). Expression of $P2X_1$ receptor protein has also been found in a variety of leukemic human cell lines, including THP1 monocytes and dibutyryl cAMP-differentiated HL-60 granulocytes (27), and $P2X_1$ receptor function has been described in PMA-differentiated HL-60 myeloid cells (36). However, until now no $P2X_1$ protein could be detected in circulating neutrophils and monocytes, so that $P2X_1$ expression was thought to be repressed at the most distal stages of phagocyte differentiation (27). Our data and a recent study describing the expression of functional $P2X_1$ ion channels in mouse peritoneal macrophages (37) question this hypothesis.

We present evidence that $P2X_1$ ion channels contribute to the control of neutrophil chemotaxis. Firstly, the selective $P2X_1$ agonists, αβMeATP and βγMeATP, are not chemoattractants by themselves but they cause random migration (chemokinesis) and amplify chemotaxis induced by endogenous (IL-8) and bacterial exogenous chemoattractants (Boyden chamber assays), as well as by living bacteria (*E. coli*) (mouse peritonitis model). Secondly, $P2X_1^{-/-}$ mice displayed impaired neutrophil recruitment in their peritoneum upon *E. coli*

injection. Thirdly, two-dimensional chemotaxis assays using collagen IV- or fibronectin-coated microslides indicated that $P2X_1^{-/-}$ neutrophils moved with diminished speed when placed in a gradient of a bacterial mimetic peptide. We also observed that static adhesion of $P2X_1^{-/-}$ neutrophils to collagen IV was impaired. The reduced migration rates of these cells could therefore be partially explained by defective adhesion dynamics required for efficient cell movement. $P2X_1^{-/-}$ neutrophils showed normal orientation in the gradient, migrated normally in Boyden chamber assays, and well polarized F-actin assembly still occurred when these cells were uniformly stimulated with W-peptide. These observations suggest that $P2X_1$ channels do not contribute to actin polymerization at the cell front and are not involved in gradient sensing. Accordingly, in Boyden chamber assays, pretreating human neutrophils with the $P2X_1$ selective antagonist, NF449, did not affect the fMLP-induced chemotaxis (supplemental Fig. S1A).[5] This is in sharp contrast with the role of $P2Y_2$ receptors that, upon activation by ATP released from cell leading edge, are required for proper cell orientation in the gradient of W-peptide (6) and contribute to actin polymerization at the front (38). In agreement with these data, we noted that UTP, acting at $P2Y_2$ receptors, was able to increase fMLP-induced chemotaxis when added together with fMLP in the bottom wells of the Boyden chamber, whereas αβMeATP could only promote chemotaxis when placed at the contact of the cells. Our findings thus emphasize differential roles for $P2Y_2$ and $P2X_1$ receptors in neutrophil migration. Since these two receptors are both activated by extracellular ATP (9), their differential effects could be related to different receptor localization (or relocalization) in membranes of migrating neutrophils and/or to the activation of distinct signaling pathways downstream from these receptors. The concentrations of ATP required to activate the two receptors in native cells may also differ. Furthermore, since $P2X_1$ receptor-mediated responses can be potentiated by $G\alpha_q$-coupled receptors (39), $P2X_1$ and $P2Y_2$ receptors could act cooperatively to promote chemotaxis.

The fact that $P2X_1^{-/-}$ neutrophils move more slowly in a gradient of chemoattractant though polarizing normally indicates that structural front-rear polarisation is not sufficient to allow efficient and rapid cell movement. Conversely, it has been shown that cells with very weak morphological polarisation move more slowly but, similarly to $P2X_1^{-/-}$ neutrophils, can chemotax with normal efficiency (40).

Signaling polarity plays an important role in determining cell movement. Cells can indeed detect differences in the concentration of chemoattractant between points on their surface (41) and translate the extracellular gradient into an intracellular derivative, encoded by the signaling networks engaged by the chemoattractant. Localized accumulation of PI3Ps is a critical signal coordinating chemotaxis or movement and depends on PI3Kγ and SHIP-1 (31, 40, 42). The study of Chen et al. proposed that ATP released from developing leading edges can act to control chemotaxis. However, the intracellular signals involved in this process remain undefined.

In our study, we found that signals elicited upon $P2X_1$ activation involved RhoA, Rho kinase and MLC phosphorylation. Several recent studies convincingly described a gradient of Rho activity along the axis of polarized neutrophils (low at the front) (43), driving myosin-based contraction at the rear (5, 44, 45). This backness pathway is mutually exclusive (in spatial terms), but partially dependent upon a frontness network, driven by the same chemoattractant and mediated via Gαi, PI3Kγ, Rac and F-actin (44). In agreement with normal morphological polarisation and F-actin assembly at the front of $P2X_1^{-/-}$ neutrophils, we could not find any evidence for PI3Kγ, Rac or Cdc42 activation downstream from $P2X_1$. Nevertheless, such frontness-backness interactions could, at least partially, explain how $P2X_1$-mediated Rho activation at the rear would promote migration elicited by a chemoattractant. Moreover, in neutrophils, actomyosin-mediated contraction at the rear of the cell seems to be a major factor in both initiating movement and forcing the cell forward (45, 46). We thus propose that $P2X_1$

activation by released ATP could trigger Rho-dependent amplification signals, facilitating membrane retraction at the receding end and possibly favouring migration-linked adhesion dynamics (47, 48). In agreement with this proposition, our time-lapse video microscopy analyses revealed more pronounced and persistent deformation of $P2X_1^{-/-}$ neutrophils and delayed detachment of trailing edge appendages as compared to wild-type cells. This observation and the fact that the selective $P2X_1$ agonist, αβMeATP, increases RhoA activity and promotes migration of wild-type neutrophils in a Rho kinase-dependent manner whereas it had no effect on $P2X_1^{-/-}$ cells, strongly suggest that the $P2X_1$-RhoA axis is required for efficient neutrophil movement, by favorizing tail retraction.

The molecular link between $P2X_1$ activation and RhoA remains unknown. RhoA is currently thought to be exclusively activated via Gα12/13 and Gαq (49) acting at guanine nucleotide exchange factors (GEFs) and GTPase-activating protein (GAPs) (50). There are at least 4 RhoA GEFs that link Gα subunits to RhoA. Among them, Lsc has been shown to be required for normal RhoA activity, polarization, migration and adhesion of fMLP-stimulated neutrophils (51). $Lsc^{-/-}$ neutrophils showed inappropriate formation and retraction of supernumerary pseudopodia. They also exhibit enhanced chemokinesis, reduced directionality and adhesion but normal chemotaxis. Except for the fact that they both show normal gradient sensing, $Lsc^{-/-}$ and $P2X_1^{-/-}$ neutrophils thus display very distinct phenotypes. Surprisingly, $Lsc^{-/-}$ neutrophils did not show any defect of tail retraction. It is thus unlikely that $P2X_1$ would signal via Lsc.

Interestingly, a recent work describes that a Ca^{2+}/calmodulin(CaM)-dependent protein kinase (CaMK) increases Rac activity through its interaction with the GEF βPak-interacting exchange factor and GIT1 in hippocampal neurons (52). Noteworthy, in platelets, $P2X_1$–triggered Ca^{2+} influx causes CaM- and MLC kinase-dependent increase of MLC phosphorylation, leading to cell shape change (26). Although we cannot rule out the

possibility that $P2X_1$ could also signal through Ca^{2+}-dependent pathways independently of RhoA, it would be interesting to determine whether Ca^{2+}- and CaMK-dependent mechanisms of RhoA activation exist in neutrophils.

In conclusion, our study indicates that $P2X_1$ ion channels contribute to the ATP-dependent control of neutrophil chemotaxis by activating signals that, in the presence of a chemoattractant, facilitate cell movement thereby enhancing chemotaxis. Further investigations are awaited to evaluate the importance of $P2X_1$-dependent signals *in vivo* and to determine whether these receptors could constitute therapeutic targets for the treatment of inflammatory diseases.

To our knowledge, this is the first evidence that $P2X_1$ ion channels contribute to cell migration. Beside the presently described role in neutrophils, it is possible that similar mechanisms apply to other $P2X_1$-expressing cell types. It is striking to note that $P2X_1$ ion channels are abundantly expressed on vascular smooth muscle cells (35, 53, 54) and on microglia (55) and might therefore contribute to various disorders related to migration of these cells that include development of restenosis, diabetic microvascular disease, chronic allograft rejection, pulmonary hypertension as well as neurological disorders.

Acknowledgements

The authors wish to thank Roel L.H.M.G. Spätjens, BSc, Cardiovascular Research Institute Maastricht, Monique Henket, GIGA Research Pneumology Unit, for expert technical assistance and Sandra Ormenese, PhD, GIGA imaging platform, for the confocal imaging.

Disclosures

The authors have no financial conflicts of interest.

References

1. Alves-Filho, J. C., A. de Freitas, F. Spiller, F. O. Souto, and F. Q. Cunha. 2008. The role of neutrophils in severe sepsis. *Shock.* 30 Suppl 1: 3-9.
2. Buffon, A., L. M. Biasucci, G. Liuzzo, G. D'Onofrio, F. Crea, and A. Maseri. 2002. Widespread coronary inflammation in unstable angina. *N. Engl. J. Med.* 347: 5-12.
3. Wipke, B. T., and P. M. Allen. 2001. Essential role of neutrophils in the initiation and progression of a murine model of rheumatoid arthritis. *J. Immunol.* 167: 1601-1608.
4. Stephens, L., L. Milne, and P. Hawkins. 2008. Moving towards a better understanding of chemotaxis. *Curr. Biol.* 18: R485-494.
5. Xu, J., F. Wang, A. Van Keymeulen, P. Herzmark, A. Straight, K. Kelly, Y. Takuwa, N. Sugimoto, T. Mitchison, and H. R. Bourne. 2003. Divergent signals and cytoskeletal assemblies regulate self-organizing polarity in neutrophils. *Cell.* 114: 201-214.
6. Chen, Y., R. Corriden, Y. Inoue, L. Yip, N. Hashiguchi, A. Zinkernagel, V. Nizet, P. A. Insel, and W. G. Junger. 2006. ATP release guides neutrophil chemotaxis via P2Y2 and A3 receptors. *Science.* 314: 1792-1795.
7. Lazarowski, E. R., R. C. Boucher, and T. K. Harden. 2003. Mechanisms of release of nucleotides and integration of their action as P2X- and P2Y-receptor activating molecules. *Mol. Pharmacol.* 64: 785-795.
8. Ralevic, V., and G. Burnstock. 1998. Receptors for purines and pyrimidines. *Pharmacol. Rev.* 50: 413-492.
9. Burnstock, G. 2007. Purine and pyrimidine receptors. *Cell Mol. Life Sci.* 64: 1471-1483.
10. North, R. A. 2002. Molecular physiology of P2X receptors. *Physiol. Rev.* 82: 1013-1067.

11. Khakh, B. S., and R. A. North. 2006. P2X receptors as cell-surface ATP sensors in health and disease. *Nature.* 442: 527-532.

12. Gu, B. J., W. Y. Zhang, L. J. Bendall, I. P. Chessell, G. N. Buell, and J. S. Wiley. 2000. Expression of P2X(7) purinoceptors on human lymphocytes and monocytes: evidence for nonfunctional P2X(7) receptors. *Am. J. Physiol. Cell Physiol.* 279: C1189-1197.

13. Mohanty, J. G., D. G. Raible, L. J. McDermott, A. Pelleg, and E. S. Schulman. 2001. Effects of purine and pyrimidine nucleotides on intracellular Ca2+ in human eosinophils: activation of purinergic P2Y receptors. *J. Allergy Clin. Immunol.* 107: 849-855.

14. Suh, B. C., J. S. Kim, U. Namgung, H. Ha, and K. T. Kim. 2001. P2X7 nucleotide receptor mediation of membrane pore formation and superoxide generation in human promyelocytes and neutrophils. *J. Immunol.* 166: 6754-6763.

15. Surprenant, A., and R. A. North. 2009. Signaling at Purinergic P2X Receptors. *Annu. Rev. Physiol*. 71: 333-359.

16. Ferrari, D., C. Pizzirani, E. Adinolfi, R. M. Lemoli, A. Curti, M. Idzko, E. Panther, and F. Di Virgilio. 2006. The P2X7 receptor: a key player in IL-1 processing and release. *J. Immunol.* 176: 3877-3883.

17. Bours, M. J., E. L. Swennen, F. Di Virgilio, B. N. Cronstein, and P. C. Dagnelie. 2006. Adenosine 5'-triphosphate and adenosine as endogenous signaling molecules in immunity and inflammation. *Pharmacol. Ther.* 112: 358-404.

18. Taylor, S. R., M. Gonzalez-Begne, S. Dewhurst, G. Chimini, C. F. Higgins, J. E. Melvin, and J. I. Elliott. 2008. Sequential shrinkage and swelling underlie P2X7-stimulated lymphocyte phosphatidylserine exposure and death. *J. Immunol.* 180: 300-308.

19. Labasi, J. M., N. Petrushova, C. Donovan, S. McCurdy, P. Lira, M. M. Payette, W. Brissette, J. R. Wicks, L. Audoly, and C. A. Gabel. 2002. Absence of the P2X7 receptor alters leukocyte function and attenuates an inflammatory response. *J. Immunol.* 168: 6436-6445.

20. Heiss, K., N. Janner, B. Mahnss, V. Schumacher, F. Koch-Nolte, F. Haag, and H. W. Mittrucker. 2008. High sensitivity of intestinal CD8+ T cells to nucleotides indicates P2X7 as a regulator for intestinal T cell responses. *J. Immunol.* 181: 3861-3869.

21. Oury, C., E. Toth-Zsamboki, C. Van Geet, C. Thys, L. Wei, B. Nilius, J. Vermylen, and M. F. Hoylaerts. 2000. A natural dominant negative P2X1 receptor due to deletion of a single amino acid residue. *J. Biol. Chem.* 275: 22611-22614.

22. Mulryan, K., D. P. Gitterman, C. J. Lewis, C. Vial, B. J. Leckie, A. L. Cobb, J. E. Brown, E. C. Conley, G. Buell, C. A. Pritchard, and R. J. Evans. 2000. Reduced vas deferens contraction and male infertility in mice lacking P2X1 receptors. *Nature.* 403: 86-89.

23. Corhay, J. L., L. Hemelaers, M. Henket, J. Sele, and R. Louis. 2007. Granulocyte chemotactic activity in exhaled breath condensate of healthy subjects and patients with COPD. *Chest.* 131: 1672-1677.

24. Oury, C., M. J. Kuijpers, E. Toth-Zsamboki, A. Bonnefoy, S. Danloy, I. Vreys, M. A. Feijge, R. De Vos, J. Vermylen, J. W. Heemskerk, and M. F. Hoylaerts. 2003. Overexpression of the platelet P2X1 ion channel in transgenic mice generates a novel prothrombotic phenotype. *Blood.* 101: 3969-3976.

25. Ho, T. T., S. D. Merajver, C. M. Lapiere, B. V. Nusgens, and C. F. Deroanne. 2008. RhoA-GDP regulates RhoB protein stability. Potential involvement of RhoGDIalpha. *J. Biol. Chem.* 283: 21588-21598.

26. Toth-Zsamboki, E., C. Oury, H. Cornelissen, R. De Vos, J. Vermylen, and M. F. Hoylaerts. 2003. P2X1-mediated ERK2 activation amplifies the collagen-induced platelet secretion by enhancing myosin light chain kinase activation. *J. Biol. Chem.* 278: 46661-46667.

27. Clifford, E. E., K. Parker, B. D. Humphreys, S. B. Kertesy, and G. R. Dubyak. 1998. The P2X1 receptor, an adenosine triphosphate-gated cation channel, is expressed in human platelets but not in human blood leukocytes. *Blood.* 91: 3172-3181.

28. Gever, J. R., D. A. Cockayne, M. P. Dillon, G. Burnstock, and A. P. Ford. 2006. Pharmacology of P2X channels. *Pflugers Arch.* 452: 513-537.

29. Evans, R. J. 1996. Single channel properties of ATP-gated cation channels (P2X receptors) heterologously expressed in Chinese hamster ovary cells. *Neurosci. Lett.* 212: 212-214.

30. Boyden, S. 1962. The chemotactic effect of mixtures of antibody and antigen on polymorphonuclear leucocytes. *J. Exp. Med.* 115: 453-466.

31. Ferguson, G. J., L. Milne, S. Kulkarni, T. Sasaki, S. Walker, S. Andrews, T. Crabbe, P. Finan, G. Jones, S. Jackson, M. Camps, C. Rommel, M. Wymann, E. Hirsch, P. Hawkins, and L. Stephens. 2007. PI(3)Kgamma has an important context-dependent role in neutrophil chemokinesis. *Nat. Cell Biol.* 9: 86-91.

32. Pomel, V., J. Klicic, D. Covini, D. D. Church, J. P. Shaw, K. Roulin, F. Burgat-Charvillon, D. Valognes, M. Camps, C. Chabert, C. Gillieron, B. Francon, D. Perrin, D. Leroy, D. Gretener, A. Nichols, P. A. Vitte, S. Carboni, C. Rommel, M. K. Schwarz, and T. Ruckle. 2006. Furan-2-ylmethylene thiazolidinediones as novel, potent, and selective inhibitors of phosphoinositide 3-kinase gamma. *J. Med. Chem.* 49: 3857-3871.

33. Hechler, B., N. Lenain, P. Marchese, C. Vial, V. Heim, M. Freund, J. P. Cazenave, M. Cattaneo, Z. M. Ruggeri, R. Evans, and C. Gachet. 2003. A role of the fast ATP-gated P2X1 cation channel in thrombosis of small arteries in vivo. *J. Exp. Med.* 198: 661-667.

34. Gachet, C. 2008. P2 receptors, platelet function and pharmacological implications. *Thromb. Haemost.* 99: 466-472.

35. Longhurst, P. A., T. Schwegel, K. Folander, and R. Swanson. 1996. The human P2x1 receptor: molecular cloning, tissue distribution, and localization to chromosome 17. *Biochim. Biophys. Acta.* 1308: 185-188.

36. Buell, G., A. D. Michel, C. Lewis, G. Collo, P. P. Humphrey, and A. Surprenant. 1996. P2X1 receptor activation in HL60 cells. *Blood.* 87: 2659-2664.

37. Sim, J. A., C. K. Park, S. B. Oh, R. J. Evans, and R. A. North. 2007. P2X1 and P2X4 receptor currents in mouse macrophages. *Br. J. Pharmacol.* 152: 1283-1290.

38. Verghese, M. W., T. B. Kneisler, and J. A. Boucheron. 1996. P2U agonists induce chemotaxis and actin polymerization in human neutrophils and differentiated HL60 cells. *J. Biol. Chem.* 271: 15597-15601.

39. Vial, C., A. B. Tobin, and R. J. Evans. 2004. G-protein-coupled receptor regulation of P2X1 receptors does not involve direct channel phosphorylation. *Biochem. J.* 382: 101-110.

40. Nishio, M., K. Watanabe, J. Sasaki, C. Taya, S. Takasuga, R. Iizuka, T. Balla, M. Yamazaki, H. Watanabe, R. Itoh, S. Kuroda, Y. Horie, I. Forster, T. W. Mak, H. Yonekawa, J. M. Penninger, Y. Kanaho, A. Suzuki, and T. Sasaki. 2007. Control of cell polarity and motility by the PtdIns(3,4,5)P3 phosphatase SHIP1. *Nat. Cell Biol.* 9: 36-44.

41. Herzmark, P., K. Campbell, F. Wang, K. Wong, H. El-Samad, A. Groisman, and H. R. Bourne. 2007. Bound attractant at the leading vs. the trailing edge determines chemotactic prowess. *Proc. Natl. Acad. Sci. U S A.* 104: 13349-13354.

42. Condliffe, A. M., K. Davidson, K. E. Anderson, C. D. Ellson, T. Crabbe, K. Okkenhaug, B. Vanhaesebroeck, M. Turner, L. Webb, M. P. Wymann, E. Hirsch, T. Ruckle, M. Camps, C. Rommel, S. P. Jackson, E. R. Chilvers, L. R. Stephens, and P. T. Hawkins. 2005. Sequential activation of class IB and class IA PI3K is important for the primed respiratory burst of human but not murine neutrophils. *Blood.* 106: 1432-1440.

43. Wong, K., O. Pertz, K. Hahn, and H. Bourne. 2006. Neutrophil polarization: spatiotemporal dynamics of RhoA activity support a self-organizing mechanism. *Proc. Natl. Acad. Sci. U S A.* 103: 3639-3644.

44. Van Keymeulen, A., K. Wong, Z. A. Knight, C. Govaerts, K. M. Hahn, K. M. Shokat, and H. R. Bourne. 2006. To stabilize neutrophil polarity, PIP3 and Cdc42 augment RhoA activity at the back as well as signals at the front. *J. Cell Biol.* 174: 437-445.

45. Sanchez-Madrid, F., and J. M. Serrador. 2009. Bringing up the rear: defining the roles of the uropod. *Nat. Rev. Mol. Cell Biol.* 10: 353-359.

46. Smith, L. A., H. Aranda-Espinoza, J. B. Haun, M. Dembo, and D. A. Hammer. 2007. Neutrophil traction stresses are concentrated in the uropod during migration. *Biophys. J.* 92: L58-60.

47. Laudanna, C., J. J. Campbell, and E. C. Butcher. 1996. Role of Rho in chemoattractant-activated leukocyte adhesion through integrins. *Science.* 271: 981-983.

48. Alblas, J., L. Ulfman, P. Hordijk, and L. Koenderman. 2001. Activation of Rhoa and ROCK are essential for detachment of migrating leukocytes. *Mol. Biol. Cell.* 12: 2137-2145.

49. Vogt, S., R. Grosse, G. Schultz, and S. Offermanns. 2003. Receptor-dependent RhoA activation in G12/G13-deficient cells: genetic evidence for an involvement of Gq/G11. *J. Biol. Chem.* 278: 28743-28749.

50. Rossman, K. L., C. J. Der, and J. Sondek. 2005. GEF means go: turning on RHO GTPases with guanine nucleotide-exchange factors. *Nat. Rev. Mol. Cell Biol.* 6: 167-180.

51. Francis, S. A., X. Shen, J. B. Young, P. Kaul, and D. J. Lerner. 2006. Rho GEF Lsc is required for normal polarization, migration, and adhesion of formyl-peptide-stimulated neutrophils. *Blood.* 107: 1627-1635.

52. Saneyoshi, T., G. Wayman, D. Fortin, M. Davare, N. Hoshi, N. Nozaki, T. Natsume, and T. R. Soderling. 2008. Activity-dependent synaptogenesis: regulation by a CaM-kinase kinase/CaM-kinase I/betaPIX signaling complex. *Neuron.* 57: 94-107.

53. Wang, L., L. Karlsson, S. Moses, A. Hultgardh-Nilsson, M. Andersson, C. Borna, T. Gudbjartsson, S. Jern, and D. Erlinge. 2002. P2 receptor expression profiles in human vascular smooth muscle and endothelial cells. *J. Cardiovasc. Pharmacol.* 40: 841-853.

54. Lewis, C. J., and R. J. Evans. 2000. Comparison of P2X receptors in rat mesenteric, basilar and septal (coronary) arteries. *J. Auton. Nerv. Syst.* 81: 69-74.

55. Xiang, Z., and G. Burnstock. 2005. Expression of P2X receptors on rat microglial cells during early development. *Glia.* 52: 119-126.

Footnotes

[1] C.L. is a Postdoctoral Researcher at the Belgian National Fund for Scientific Research and got a fellowship from the Simone and Cino del Duca Foundation, K.F. was supported by the Belgian Science Policy (IAP 6/18), C.F. was supported by a F.R.I.A. ("Fond pour la recherche industrielle et agricole") fellowship. C.O. is a Research Associate at the Belgian National Fund for Scientific Research. This work was supported by the Belgian National Fund for Scientific Research (Project n°1.5.203.06), Belgian Science Policy (IAP6/18) and by the "Fondation Léon Frédéricq" and "Fonds spéciaux pour la recherche" (Project n° I-05/02) of the University of Liège, Belgium.

[2] C.L. and K.F. contributed equally to this work.

[3] Address correspondence and reprint requests to Dr Cécile Oury, PhD, University of Liège GIGA-Research Human Genetics Unit, Tour GIGA B34, Avenue de l'Hôpital 1, B-4000 Liège, Belgium. E-mail address: cecile.oury@ulg.ac.be.

[4] Abbreviations used in this paper: αβMeATP, alpha,beta-methylene ATP; βγMeATP, beta,gamma-methylene ATP; CI, chemotactic index, MLC, myosin light chain; PI3Ps, 3'-phosphoinositol lipids; RT, room temperature; WT, wild-type.

[5] The online version of this article contains supplemental material.

Figure legends

FIGURE 1. Human neutrophils express functional $P2X_1$ channels. *A,* Western blotting detection of $P2X_1$ proteins in neutrophil or platelet protein extracts. *B,* Whole cell currents recorded at -70mV holding potential. The average cell capacitance of human peripheral neutrophils was 2.1 ± 1.0 pF (mean ± SD). Representative traces of inward currents induced by optimal concentrations of αβMeATP (10μM) and βγMeATP (10μM). The histograms depict current density. Averaged data are from at least three independent experiments with neutrophils of different individuals.

FIGURE 2. αβMeATP induces random migration of human peripheral neutrophils and enhances chemotaxis. Boyden chamber assays on human peripheral neutrophils. *A,* αβMeATP (10 μM) or HBSS (neutrophil resuspension buffer), *B,* IL-8 (100 ng/ml), or *C-E,* fMLP (100nM). *D,* αβMeATP (10 μM) or *E,* UTP (10 μM) were combined or not with fMLP (100 nM) and placed in the bottom wells of the chamber, as indicated below the solid bars. The "+" or "-" symbols above the solid bars indicate that neutrophils were pre-stimulated or not with the indicated agonists (αβMeATP in *A-D*, or UTP in *E*) for 1 min prior to addition to the upper wells of the chamber. Averaged data are from at least three independent experiments with neutrophils of different individuals. *A-C*, *p<0.05, **p<0.01, ***p<0.001 *vs* absence of αβMeATP in the upper wells. *E,* *p<0.05 *vs* absence of UTP.

FIGURE 3. Role of RhoA-Rho kinase pathway in αβMeATP-triggered migration of human neutrophils. *A-B,* RhoGTPase activities assessed by GST-pull down assays. Human neutrophils were stimulated with αβMeATP (10μM) for the indicated times. Immunoblots depicting GST-bound and total GTPase levels are shown. *A,* A representative immunoblot of

GST-bound and total RhoA and levels of GST-bound RhoA normalized to the signal detected in the absence of αβMeATP are shown. *B,* Representative immunoblots of GST-bound and total Rac1, Rac2 and Cdc42. *C,* Representative immunoblot of phosphorylated (P-MLC) and total myosin light chain (MLC) in neutrophils stimulated with αβMeATP (10μM) for the indicated times. Bottom panel, results of band quantification. Levels of P-MLC were normalized to the signal detected in the absence of αβMeATP. *D,* Boyden chamber assays. αβMeATP-treated neutrophils were preincubated or not with the Rho kinase inhibitors, Y27632 (5μM) or H1152 (1μM) for 15 min. αβMeATP (10μM) was added in the bottom wells. Cell migration in the presence of HBSS is also shown (control). *E,* fMLP (100 nM) was placed in the bottom wells of the Boyden chamber. Neutrophils preincubated or not with the Rho kinase inhibitor Y27632 (5 μM) were placed in the upper wells in the presence or absence of αβMeATP (10 μM), as indicated. Data represent the means ± SD of at least three independent experiments with neutrophils of different individuals. *A,* *$p<0.05$ *vs* control. *C,* **$p<0.01$ *vs* control. *D,* **$p<0.01$ *vs* HBSS control, $^{\#}p<0.05$ *vs* αβMeATP. *E,* ***$p<0.001$ *vs* fMLP alone (control), $^{\#\#\#}p<0.001$ *vs* αβMeATP.

FIGURE 4. Characterization of $P2X_1^{-/-}$ neutrophils. Whole cell currents recorded at -70mV holding potential. The average cell capacitance of mouse peritoneal neutrophils was 1.7 ± 0.3 pF (mean ± SD). Representative traces of αβMeATP (10μM) and βγMeATP (10μM) induced inward currents in WT and $P2X_1^{-/-}$ peritoneal neutrophils.

FIGURE 5. Chemotaxis and RhoA signaling in wild-type and $P2X_1^{-/-}$ neutrophils. *A-B,* Boyden chamber assays. *A,* W-peptide (100 nM) was placed in the bottom wells of the chamber. Wild-type (WT) and $P2X_1^{-/-}$ peritoneal neutrophils were pretreated or not (control) with αβMeATP (10μM) for 1 min prior being placed in the upper wells. *B,* WT neutrophils

were preincubated or not with the Rho kinase inhibitors H1152 (1 μM) or Y27632 (5 μM) before pretreatment with αβMeATP, as indicated. Migrating neutrophils were counted after 1 hour. Averaged data are from at least three independent experiments with neutrophil pools from three mice. *A,* *p<0.05 *vs* absence of αβMeATP (control). *B,* **p<0.01 *vs* absence of αβMeATP (control), $^{###}$p<0.001 *vs* absence of inhibitors. *C,* RhoA GTPase activity was assessed in WT and $P2X_1^{-/-}$ neutrophils stimulated with αβMeATP (10μM) for the indicated times. Numbers below the immunoblots represent the fold-increase of RhoA activity normalized to the signal detected in the absence of αβMeATP. Data are representative of two independent experiments with neutrophil pools from 8 animals.

FIGURE 6. Impaired static adhesion, diminished speed and increased time to trailing edge retraction for $P2X_1^{-/-}$ neutrophils. *A-C,* Study of WT and $P2X_1^{-/-}$ neutrophil two-dimensional migration using collagen IV-coated Ibidi chemotaxis microslides. *A,* Migration speed. *B,* Representative image captured at 60 min showing several $P2X_1^{-/-}$ neutrophils with a persistent trailing edge (white arrows). *C,* Averaged circularity ratio of cells during the time course of three independent experiments. Between 40 and 100 cells were assigned scores. *p<0.05, **p<0.01. *D,* Static cell adhesion assay. Peritoneal neutrophils were placed onto collagen IV-coated wells for 15 min and the percentage of adherent cells was determined. Averaged data are from three independent experiments with neutrophil pools from two animals. *p<0.05 *vs* WT.

FIGURE 7. Normal F-actin polymerisation in $P2X_1^{-/-}$ neutrophils uniformly stimulated with W-peptide. Confocal images of murine peritoneal neutrophils adhered to collagen IV and incubated with 100 nM W-peptide for the indicated times before labeling with Alexa 488-labeled phalloidin (magnification X210).

FIGURE 8. $P2X_1$ promotes neutrophil recruitment *in vivo* in a model of *E. coli*-induced peritonitis. *A,* WT mice injected intraperitoneally with either PBS (vehicle) or *E.coli*. These mice were injected intraperitoneally with αβMeATP or vehicle (control) prior to and after *E. coli* injection. First treatment was administered 15 min before *E.coli*/vehicle; second and third treatments were given after 1 and 2 hours, respectively. Mice were sacrificed after 3 hours. Neutrophils were counted in the peritoneal lavages. *B,* WT and $P2X_1^{-/-}$ mice injected intraperitoneally with PBS (vehicle) or *E.coli*. *A-B,* Averaged data are from three independent experiments performed with groups of four to six mice. *A,* *p<0.05 *vs* control; #p<0,05 *vs* vehicle, ###p<0,001 *vs* vehicle. *B,* *p<0.05 WT *E.coli vs* $P2X_1^{-/-}$ *E.coli*; #p<0,05 *vs* vehicle, ###p<0,001 *vs* vehicle

Lecut et al., Figure 1

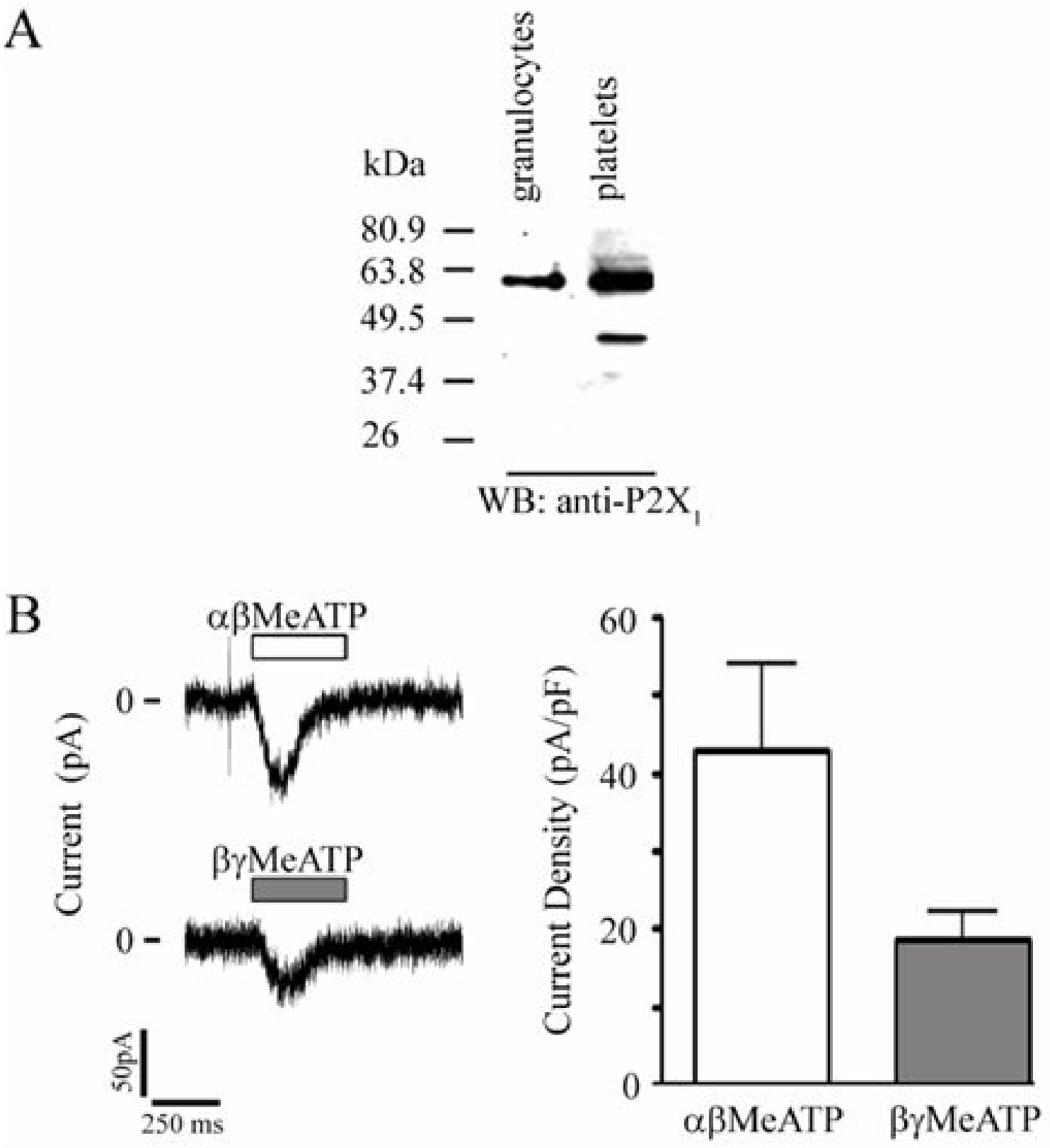

Lecut et al., Figure 2

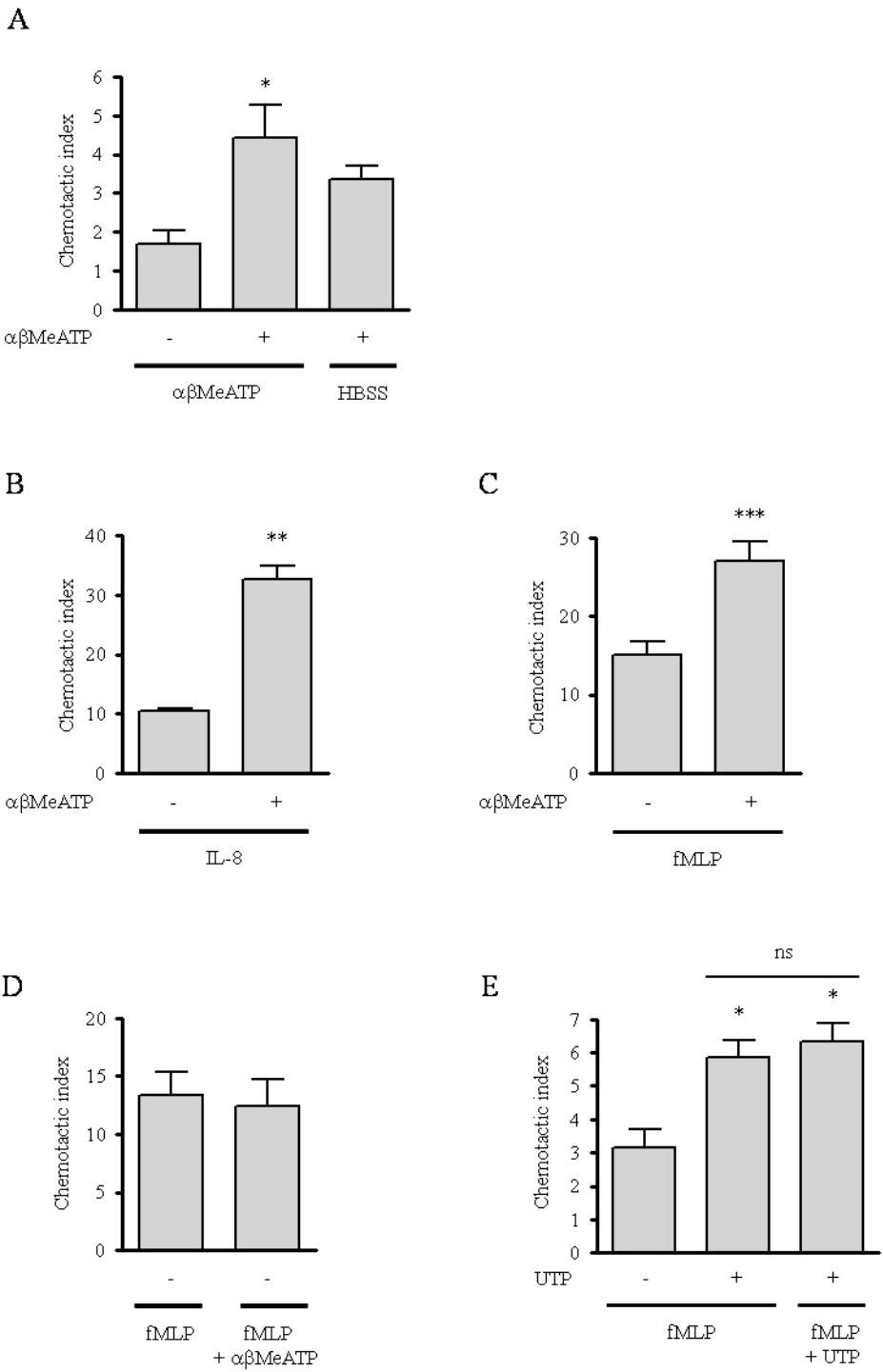

Lecut et al., Figure 3

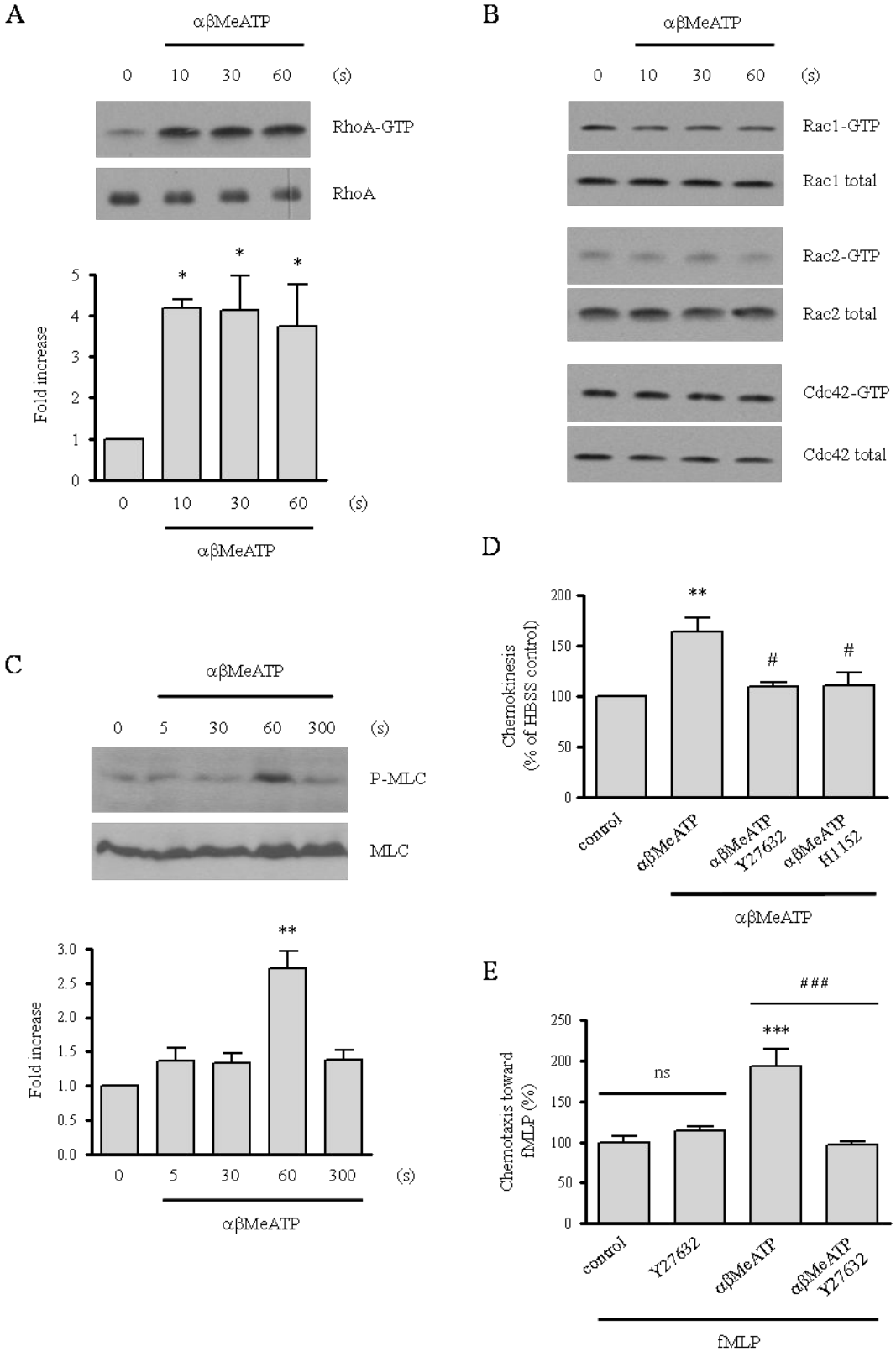

Lecut et al., Figure 4

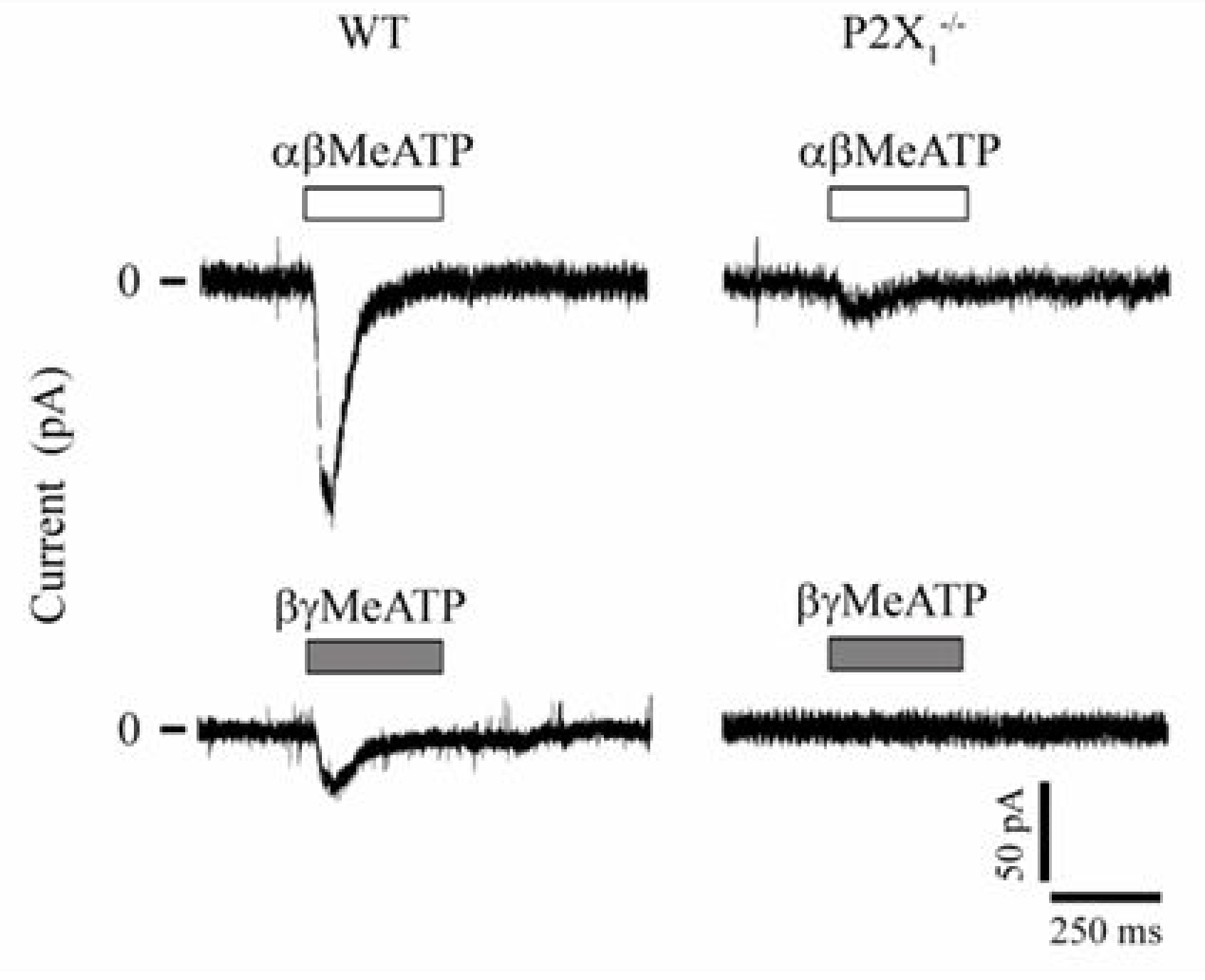

Lecut et al., Figure 5

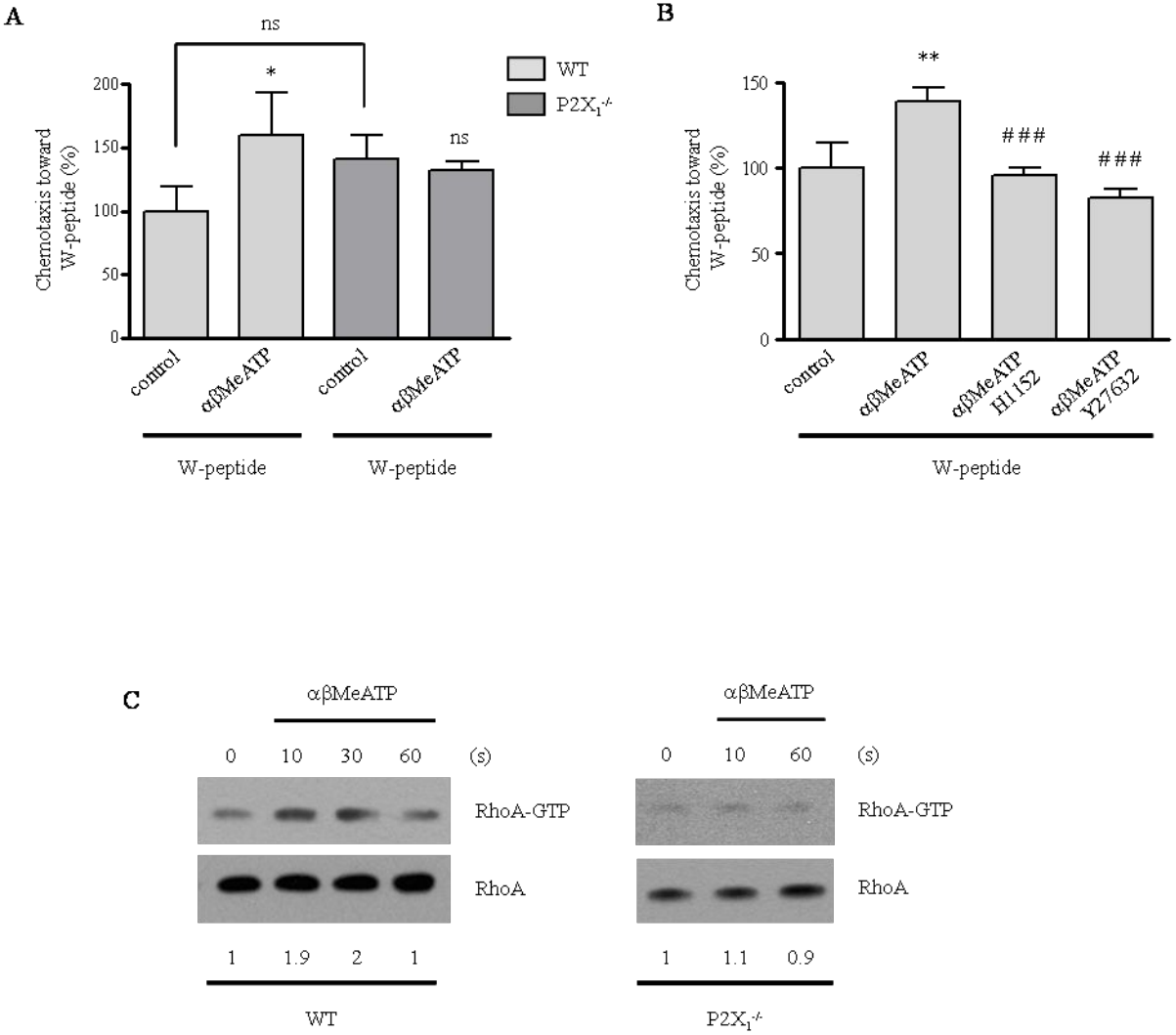

Lecut et al., Figure 6

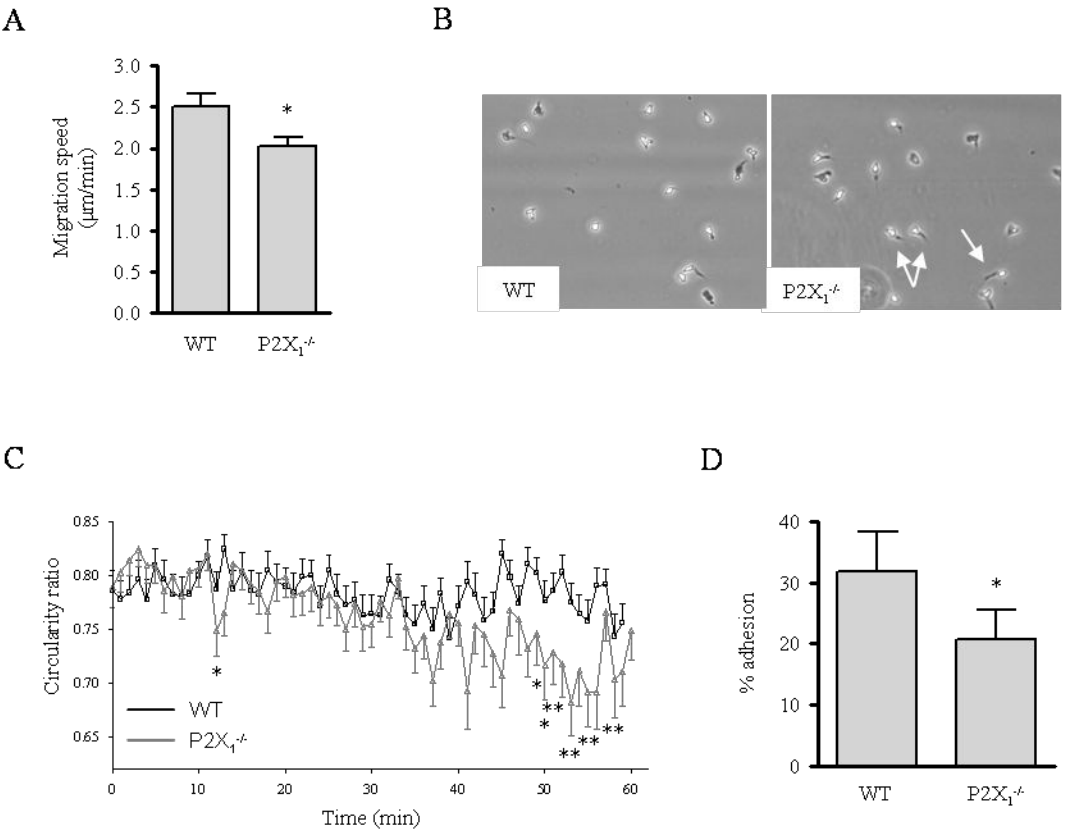

Lecut et al., Figure 7

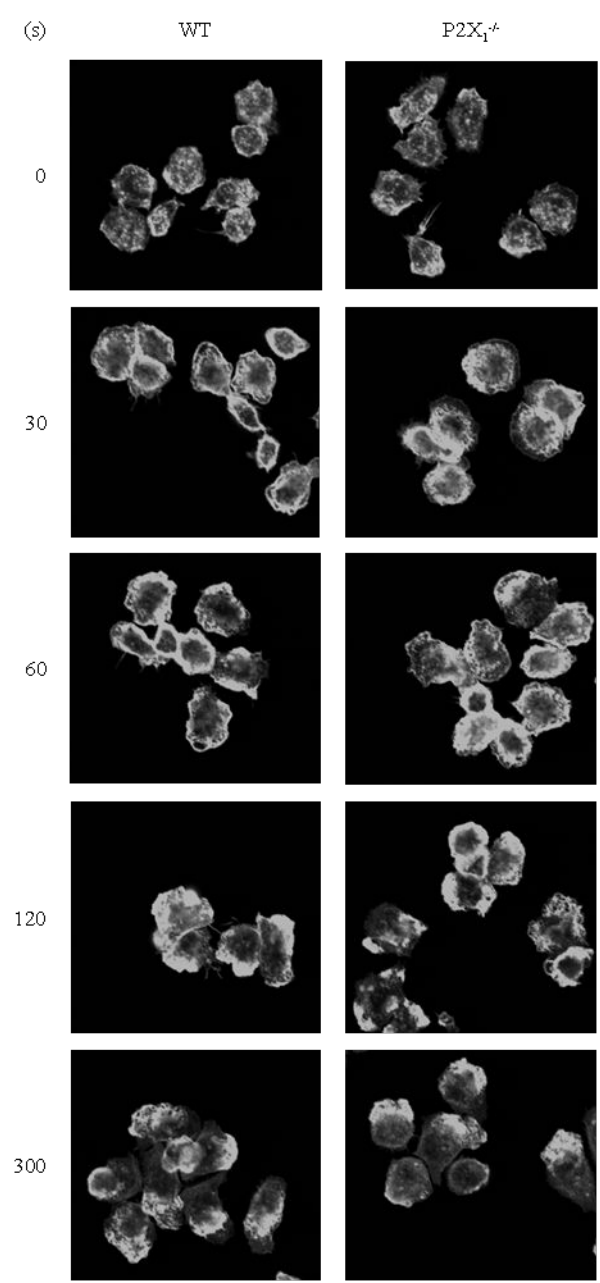

Lecut et al., Figure 8